JOURNAL OF RAMAN SPECTROSCOPY, VOL. 29, 291–295 (1998)

Comparative Determination of Absolute Raman Scattering Efficiencies and Application to GaN

I. Loa,[1]* S. Gronemeyer,[1] C. Thomsen,[1] O. Ambacher,[2] D. Schikora[3] and D. J. As[3]
[1] Institut für Festkörperphysik, Technische Universität Berlin, D-10623 Berlin, Germany
[2] Walter-Schottky-Institut, Technische Universität München, D-85746 Garching, Germany
[3] Universität Paderborn, FB 6-Physik, D-33098 Paderborn, Germany

Absolute Raman scattering efficiencies for first-order light scattering of optical zone-center phonons were determined for cubic and hexagonal GaN. An improved method for the determination of scattering efficiencies by comparative measurement with a standard substance such as BaF_2 was used to minimize the experimental errors substantially. © **1998 John Wiley & Sons, Ltd.**

J. Raman Spectrosc. **29**, 291–295 (1998)

INTRODUCTION

In recent years, GaN has received considerable attention as a promising material for applications in optoelectronics in the blue and ultraviolet spectral range. Especially the recent success in using GaN for laser diodes has given rise to the possibility of satisfying even commercial requirements in the near future. Since it became possible to grow both hexagonal (α-GaN) and cubic GaN (β-GaN) layers of good quality and sufficient size, great efforts have been made to investigate their optical properties.

Absolute cross-sections for Raman scattering and their wavenumber dependence are of great importance as a stringent test of the theories used to describe the scattering mechanisms.[1,2] It is also common practice to deduce from these absolute values quantitative results for the magnitude of deformation potentials and electron–phonon coupling constants.[3,4] In the case of GaN they would provide important data for checking the band structure calculations which nowadays are carried out extensively. Likewise, absolute scattering efficiencies could yield an easy and reliable method to determine quantitatively minority phases of α-GaN in β-GaN by means of Raman spectroscopy.[5] Absolute values are also of interest as a basis for the calibration of two-photon absorption cross-sections or other nonlinear optical parameters such as the third-order nonlinear susceptibility.[6]

Several methods are used for the experimental determination.[7] Because any truly absolute measurement of a cross-section is charged with the problem of having to take into account the optical characteristics of all the components used in the experiment, comparative methods are usually preferred. In this work we determined the scattering efficiency of nearly all optical zone center phonons for several samples of hexagonal and cubic GaN by comparison with the standard substances BaF_2 and CaF_2 at an incident photon energy of 2.41 eV.

* Correspondence to: I. Loa, Max-Planck-Institut für Festkörperforschung, Heisenbergstr. 1, D-70569 Stuttgart, Germany.
E-mail: ingor@physik.tu-berlin.de

THEORY

The relationship between the differential Raman cross-section $d\sigma$ that equals the ratio of scattered to incident power per unit solid angle Ω and the commonly used scattering efficiency S is given by

$$\frac{dS}{d\Omega} = \frac{1}{V}\frac{d\sigma}{d\Omega} \tag{1}$$

where V denotes the effective scattering volume, i.e. the volume where the scattering processes take place and where the detected signal comes from. The efficiency S is given with dimensions $m^{-1}\ sr^{-1}$. In the case of Stokes scattering it is[7]

$$\frac{dS_S}{d\Omega} = \left(\frac{\omega_s}{c}\right)^4 \frac{N\hbar}{2M_R\,\omega_v}(n_0+1)\sum_i^{\text{optical}} |\hat{\mathbf{e}}_s \mathbf{R}_i \hat{\mathbf{e}}_L|^2 \tag{2}$$

where ω_s is the angular frequency of the scattered light, ω_v that of the phonon, c the speed of light in vacuum, M_R the reduced mass of the vibrating atoms, N the number of primitive cells per unit volume and n_0 the Bose–Einstein population factor evaluated at the wavenumber of the phonon. The polarizations of incident and scattered light are described by the dimensionless unit vectors $\hat{\mathbf{e}}_L$ and $\hat{\mathbf{e}}_s$. The summation is carried out over all optical phonons i that are represented by their Raman tensors $\mathbf{R}_i$. If the symmetry of the crystal concerned is known, it is possible to determine the magnitude of the entries of the Raman tensors, the so-called Raman polarizabilities of the material.

In practice, the scattered power P_s is proportional to the area A under the peak in the Raman spectrum of the phonon in question per integration time t:

$$P_s \propto \frac{A}{t} \tag{3}$$

Assuming the scattering process to be isotropic in the solid angle Ω, the relationship between the power P_s

CCC 0377–0486/98/040291–05 $17.50

Received 10 October 1997
Accepted 5 January 1998

scattered in Ω per volume V and the scattering efficiency S_S becomes:

$$\frac{dS_S}{d\Omega} \propto \frac{P_s}{VP_L\Omega} \tag{4}$$

where P_L is the incident laser power that induces the scattering processes in the crystal. All quantities require corrections with respect to refraction, reflection and absorption of incident and scattered radiation. Experimentally, the scattered light is collected from an *external* solid angle Ω_e, which is given by the numerical aperture of the collecting lens. Considering refraction at the sample surface, one obtains an *internal* solid angle Ω_i which is to be used in Eqn (4). In the case of small angles it can be approximated by

$$\frac{\Omega_i}{\Omega_e} = \left(\frac{n_a}{n_s}\right)^2 \tag{5}$$

where n_a and n_s denote the refractive indices of air and sample, respectively.

The reflection losses at the sample surface can be evaluated using the usual Fresnel equation for the normal-incidence reflectivity. Taking into account that reflection occurs for both the incident and the scattered light and incorporating the solid-angle correction according to Eqn (5), one obtains a total correction factor

$$C_n = \left(\frac{n_s}{n_a}\right)^2\left[1 - \left(\frac{n_s - n_a}{n_s + n_a}\right)^2\right]^{-2} = \frac{1}{16}(n_s + 1)^4 \tag{6}$$

with $n_a = 1$. Since this correction is proportional to the fourth power of n_s, it will become one of the principal sources of experimental error.

It seems common practice to approximate the scattering volume V by a simple cylinder within which the light scattering is assumed to be homogeneous. Its diameter is approximated by the laser spot size in terms of a Gaussian beam waist. Depending on the sample thickness, the cylinder height is approximated by either the Rayleigh length of the focused laser beam or the sample thickness in the case of thin samples. This procedure appears as a source of substantial error for the following reasons. Such a definition of the scattering volume is rather arbitrary in that it simply uses quantities that are easily accessible in the context of Gaussian beams. Even if one properly took into account the propagation of the laser light within the sample, it would still require accurate evaluation of the beam properties—which itself is not a trivial task—and would not at all take into account the characteristics of the collecting optics. Provided that samples of similar thickness and optical properties are used, this might be acceptable. However, when comparing thin films as in the case of GaN with standards in the form of bulk crystals, this practice becomes a major source of uncertainty. We therefore propose the following procedure to overcome all of these problems.

METHODS

The basic idea is first to sample both the excitation strength of the laser beam and the collection efficiency of the optical system at different distances from the laser focus. Then, this experimentally determined characteristic is integrated over the thickness of the sample to be investigated, which results in a numerical model for the depth profile. This model is then compared with a measured depth profile. Doing so for two samples allows one to evaluate the relative scattering efficiencies fairly accurately. This method also overcomes the need for exact and reproducible focusing on to the surfaces of different samples and any evaluation of the beam properties.

The first task, measuring the characteristics of the excitation and collection efficiency, can easily be achieved by moving a very thin sample along the laser beam through the laser focus, taking a Raman spectrum at each point and using the integrated intensity of a Raman peak as a measure. In our experiments, the Raman spectra were recorded in backscattering geometry as illustrated in Fig. 1(a). We commonly used a 400 nm ZnSe layer grown on GaAs, which gives good results owing to the large scattering cross-section of ZnSe. We also used a 1 μm film of GaN grown on GaAs, which reproduced the profile obtained with ZnSe very well. We noticed, however, that films grown on transparent substrates are not as well suited, as reflections from the back surface of the substrate can cause some distortion of the caracteristic. Figure 1(b) shows a series of Raman spectra of a 1 μm film of cubic GaN taken at different sample positions x. It illustrates the varying excitation and collection efficiencies as the

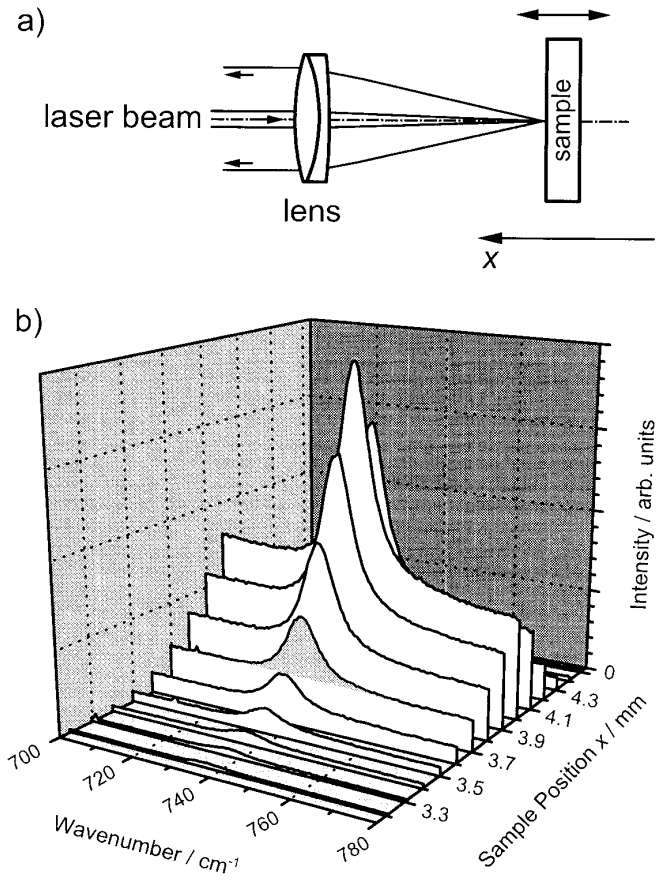

Figure 1. (a) Raman spectra recorded in backscattering geometry with the sample being displaced along the optical axis. (b) Series of Raman spectra of cubic GaN (1.25 μm layer) for various sample positions x.

sample is moved through the laser focus. Only the integrated intensity of the phonon peak, marked by the gray area of the curve at $x = 3.7$ mm, was used as a measure for the characteristic, thus eliminating the influence of the luminescence background. The resulting excitation characteristic is shown in Fig. 2(a), where the data points correspond to the spectra in Fig. 1(b).

The second step is to model the depth profile for the samples to be investigated. In principle, one needs to integrate the measured charactersitic $C_0(x)$ of the thin reference sample over the thickness d of the sample in question, which result in a model C_s. Taking into account refraction at the sample surface we obtain

$$C_s(x_0) = \int_0^d R_s\, C_0(x_0 + x/n_s)\, dx \qquad (7)$$

where x_0 is the position of the sample, n_s its refractive index and R_s the relative scattering efficiency. In other words, $C_s(x_0)$ models the variation of the Raman intensity when the spectrum is taken with the sample at different positions x_0. The integration can be done either numerically or analytically. In the latter case one needs to represent the measured characteristic by some analytical function for which the integration can be performed. To facilitate some curve fitting in the final step, we represented our experimental characteristic by a sum of Gaussian functions for which Eqn (7) can be evaluated analytically:

$$C_0(x) = \sum_i A_i \exp\left[-(x - x_i)^2/2\gamma_i^2\right]$$

$$C_s(x_0) = \sum_i R_s n_s A_i \gamma_i \sqrt{\pi/2} \times \left\{\mathrm{erf}\left[\frac{d + (x_0 - x_i)n_s}{\sqrt{2}\, n_s \gamma_i}\right] - \mathrm{erf}\left(\frac{x_0 - x_i}{\sqrt{2}\,\gamma_i}\right)\right\} \qquad (8)$$

It should be noted that the specific choice of Gaussian functions for the representation of $C_0(x)$ was arbitrary but guided by convenience. It is only important to find a representation of the measured profile for which the integration in Eqn (7) can be performed so that its analytical result [Eqn (8)] can be used with a conventional least-squares fit.

Finally, this model $C_s(x_0)$ can be compared with a measured profile. If d and n_s are known, the relative scattering efficiency R_s is the only adjustable parameter. It can be determined easily by fitting $C_s(x_0)$ to the experimental data by a standard least-squares procedure. Figure 2 illustrates the whole procedure. Figure 2(a) shows the measured characteristic $C_0(x)$ together with its representation by a sum of four Gaussians. In Fig. 2(b), the parameter R_s was adjusted to fit optimally the measured depth profile $C_s(x_0)$ of a 1 mm BaF_2 sample. The deviation for large x_0 values is due to reflections at the back surface of the sample. Applying this procedure to both the reference sample and the crystal to be examined, their relative scattering efficiency can be determined very accurately and without making any assumptions regarding the propagation of the laser beam and the collection characteristics of the spectrometer. Of course, corrections regarding refraction [Eqn (5)] and reflection with the known indices of refraction are still required.

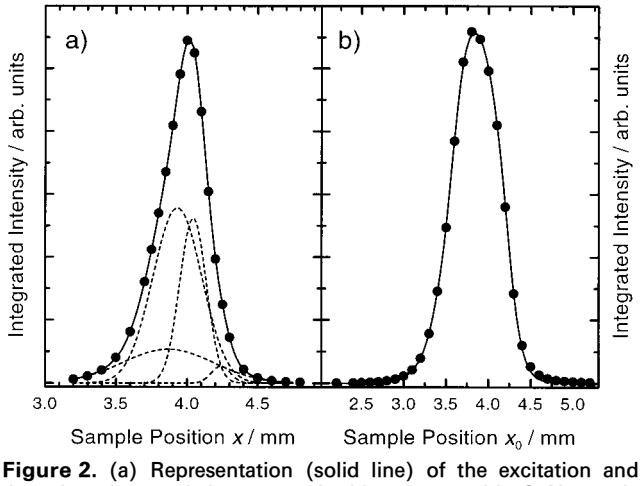

Figure 2. (a) Representation (solid line) of the excitation and detection characteristic measured with a 1 μm cubic GaN sample (dots) by a sum of four Gaussian functions (dashed lines). (b) Experimental depth profile of a 1 mm BaF_2 sample (dots) and the result of the model in Eqn (8) (solid line).

EXPERIMENTAL

Most of the experiments were carried out using a macro-Raman experimental set-up. Only for comparative measurements within the same sample did we prefer a micro-Raman set-up. It was used to determine phonon cross-sections in scattering geometries, which are not accessible with the standard set-up. Within one sample, direct comparison of different phonon modes is possible provided that at least one mode can be used for reference in the investigated geometries.

An argon/krypton ion laser[9] was used for excitation at 514 nm at a power level of about 20 mW (<1 mW) for the macro- (micro-) Raman set-up. Focusing of the laser beam and collection of the scattered light was done in the macro-Raman set-up by a photo objective with a focal length of 50 mm. For the micro-Raman set-up we used a 100 × microscope objective of numerical aperature 0.95. All spectra were recorded in backscattering geometry using a triple grating spectrometer.[10]

The standards were (111)-cleaved BaF_2 and CaF_2 single crystals with a thickness of 0.94 and 1.7 mm, respectively. A 400 nm ZnSe/GaAs layer was used for sampling of the excitation and collection characteristic. Four GaN samples were investigated. Two of them were hexagonal (001) films grown on sapphire by MOCVD[11] and MBE[12] with a thickness of 2.1 and 3.4 μm, respectively; we did not find significant differences between these two. The latter film and a 350 μm hexagonal sample were used for measurements perpendicular to the crystal c-axis in order to examine phonons that can be observed only in this configuration. Finally, a 1.25 μm cubic film with a (001) surface grown on GaAs[13] was investigated.

Table 1 summarizes the refractive indices at an excitation energy of 2.41 eV that were used for the necessary corrections. The error intervals consider mainly the inaccuracy of the values found in the literature and a

Table 1. Refractive indices of the investigated materials at a photon energy of 2.41 eV

Material	n	Ref.
α-GaN	2.44 ± 0.05	14
β-GaN	2.36 ± 0.10	15
BaF_2	1.47 ± 0.01	16
CaF_2	1.44 ± 0.01	16

general dependence of optical properties on purity and quality of the investigated samples.[17] Variations of the optical parameters with phonon energies were negligible.

RESULTS AND DISCUSSION

Table 2 summarizes the measured relative and absolute Raman cross-sections for three samples in various scattering geometries. The absolute scattering efficiencies of the E_2(high) and A_1(LO) phonons were measured in a direct comparison of the 3.4 μm α-GaN sample with BaF_2 as outlined above. The values are based on a scattering efficiency $dS_S/d\Omega = (0.28 \pm 0.05) \times 10^{-5}$ m^{-1} sr^{-1} of BaF_2 [7] for backscattering on the (111) surface with polarizations $\mathbf{e}_L = \mathbf{e}_s$. The cross-sections of the phonons in other configurations were obtained by internal comparison with the E_2(high) mode, which can be observed in both the $z(\ldots)\bar{z}$ and the $x(\ldots)\bar{x}$ configuration. For the determination of the absolute $x(\ldots)\bar{x}$ quantities we assumed the scattering efficiency of the E_2(high) mode to be the same in both configurations as is predicted by the symmetry properties of the crystal. In addition, the scattering cross-section of the T_2(LO) phonon in cubic GaN was determined by direct comparison with BaF_2.

It should be noted that although the E_2(low) and E_2(high) modes in hexagonal GaN have the same symmetry, we found their intensity ratio to differ in the $z(xx)\bar{z}$ and the $z(yx)\bar{z}$ configuration. Since we cannot give a conclusive explanation of this observation, Table 2 also reports a set of relative scattering efficiencies for the 350 μm sample. These data are given to mark the range of uncertainty that is due to sample dependence.

With regard to the detection of minority phases in hexagonal and cubic GaN, we also determined the scattering efficiency of the cubic T_2(LO) mode relative to the hexagonal E_2(high) and A_1(TO) modes: $S_S[T_2(LO)]/S_S[E_2(high)] = 1.6 \pm 0.4$ and $S_S[T_2(LO)]/S_S[A_1(TO)] = 3.8 \pm 1.0$.

The errors given in Table 2 take into account systematic errors due to the uncertainties of the indices of refraction and sample thicknesses and also the statistical error of the relative scattering efficiency R_s derived from the depth-profile fit. The errors of the absolute scattering efficiencies listed in Table 2 include the 18% error of the absolute scattering cross-section of the reference material BaF_2 on which this comparative measurement is based. It is the largest error contribution. The second most important single source of error in all cases is the uncertainty of the refractive index used for the reflection loss and solid angle correction according to Eqn (6) because of its fourth-power dependence. When more accurate values for either the refractive indices or the absolute scattering efficiency of BaF_2 are available, more accurate cross-sections of GaN can be deduced based on the relative scattering efficiencies listed in Table 2.

In order to demonstrate the advantage of the proposed method, we also evaluate the scattering efficiency of the α-GaN E_2(high) mode relative to BaF_2 using the conventional procedure, i.e. approximating the scattering volume by a cylinder as described above. This will generally lead to an over-estimation of the scattering volume of the thick standard sample since, compared with a thin sample, light scattered from the out-of-focus regions is detected with lower efficiency. Because of this, the scattering cross-section of the reference material will be under-estimated, finally resulting in too large a value of the absolute cross-section of the sample in question. Specifically, the Rayleigh length was

Table 2. Relative and absolute scattering cross-sections of hexagonal and cubic GaN at a photon energy of 2.41 eV[a]

Sample	Raman mode	Polarization (Porto)	Scattering efficiency: Relative to BaF_2	Scattering efficiency: Relative to hexagonal GaN E_2(high)	Scattering efficiency: Absolute 10^{-5} m^{-1} sr^{-1}
α-GaN (3.4 μm)	E_2(high, 566 cm^{-1})	$z(xx)\bar{z}$	13.5 ± 1.5	1	3.8 ± 1.1
	E_2(low, 143 cm^{-1})	$z(xx)\bar{z}$	[0.26 ± 0.02]	(1.91 ± 0.02) × 10^{-2}	[0.07 ± 0.02]
	E_2(low, 143 cm^{-1})	$z(yx)\bar{z}$	[0.33 ± 0.04]	(2.42 ± 0.02) × 10^{-2}	[0.09 ± 0.03]
	A_1(LO, 735 cm^{-1})	$z(xx)\bar{z}$	5.8 ± 0.7	0.43 ± 0.01	1.6 ± 0.5
	A_1(TO, 531 cm^{-1})	$x(yy)\bar{x}$	[7.3 ± 1.2]	0.54 ± 0.03	[2.1 ± 0.7]
	E_1(TO, 558 cm^{-1})	$x(zy)\bar{x}$	[8.1 ± 1.6]	0.60 ± 0.05	[2.2 ± 0.9]
α-GaN (350 μm)	A_1(TO, 531 cm^{-1})	$x(yy)\bar{x}$	—	0.47 ± 0.01	—
	A_1(TO, 531 cm^{-1})	$x(zz)\bar{x}$	—	2.1 ± 0.1	—
	E_1(TO, 558 cm^{-1})	$x(zy)\bar{x}$	—	0.79 ± 0.04	—
	E_1(TO, 558 cm^{-1})	$x(yz)\bar{x}$	—	0.86 ± 0.10	—
β-GaN	T_2(LO, 737 cm^{-1})	$z(x'x')\bar{z}$	22 ± 4	1.6 ± 0.4	6 ± 2

[a] Values in square brackets were determined indirectly by comparison with the E_2(high) mode measured on the same crystal surface.

determined as 1.1 mm, and the BaF_2 sample has a thickness of 0.94 mm, so that the scattering volume would be expected to be limited by the latter. As can be seen from Fig. 2(b), the scattering volume is effectively limited by the characteristics of the collecting optics with a depth-of-focus of *ca.* 0.7 mm, i.e. significantly smaller than the sample thickness. Consequently, even in the best-case situation (focusing into the center of the 0.94 mm BaF_2 sample), the result obtained by the conventional method is too large by a factor of 1.7.

One should also consider the possible impact of interference effects due to reflections at the sample surfaces. It is not a specific problem in the proposed method but applies to any measurement of Raman intensities. For the present study, we could exclude such effects by comparison of the results for samples with different thickness in the case of our hexagonal GaN films, where no differences were found. In the case of the cubic GaN sample, interference effects could not occur because of its microscopically rough surface.

We also used CaF_2 as a standard material. By comparison with BaF_2 we determined the absolute cross-section of CaF_2 as $dS_S/d\Omega = (0.065 \pm 0.017) \times 10^{-5}$ m^{-1} sr^{-1}. The relative scattering efficiency of CaF_2 and BaF_2 is $S_S(CaF_2)/S_S(BaF_2) = 0.232 \pm 0.019$.

In conclusion, an improved method for the comparative measurement of absolute Raman scattering cross-sections was developed. It was shown that the conventional technique can lead to severe overestimation of the deduced Raman cross-sections. The new method was employed to determine the scattering efficiencies of most zone-center optical phonons in hexagonal and cubic GaN. For the quantitative determination of hexagonal minority phases in cubic GaN, we directly measured the relative scattering cross-sections of the cubic T_2(LO) mode in comparison with the hexagonal E_2(high) and A_1(TO) modes.

Acknowledgements

We thank H. Siegle, L. Filippidis and A. Kaschner for helpful discussions.

REFERENCES

1. M. H. Grimsditch and M. Cardona, in *Physics of Semiconductors*, edited by B. Wilson, p. 639. Institute of Physics, London (1978).
2. W. Richter, *Springer Tracts Mod. Phys.* **78**, 121 (1976).
3. C. A. Arguello, D. L. Rousseau and S. P. S. Porto, *Phys. Rev.* **181**, 1351 (1969).
4. M. Cardona, M. H. Grimsditch and D. Olego, in *Light Scattering in Solids I*, edited by L. Birman and Z. Cummins, pp. 639. Springer, Berlin (1979).
5. H. Siegle, L. Eckey, A. Hoffmann, C. Thomsen, B. K. Meyer, D. Schikora, M. Hankeln and K. Lischka, *Solid State Commun.* **96**, 943 (1995).
6. Y. Prior and H. Vogt, *Phys. Rev. B* **19**, 1351 (1979).
7. M. Cardona, in *Light Scattering in Solids II*, edited by M. Cardona and G. Güntherodt, pp. 19. Springer, Berlin (1982).
8. M. H. Grimsditch and A. K. Ramdas, *Phys. Rev. B* **11**, 3139 (1975).
9. *Innova 70 Spectrum*. Coherent, Palo Alto, CA.
10. *XY800*. Dilor, France.
11. O. Ambacher, R. Dimitrov, D. Lentz, T. Metzger, W. Rieger and M. Stutzmann, *J. Cryst. Growth* **167**, 1 (1996).
12. H. Angerer, O. Ambacher, R. Dimitrov, T. Metzger, W. Rieger and M. Stutzmann, *MRS Internet J. Nitride Semiconductor Res.* **1**, 15 (1996).
13. D. Schikora, M. Hankeln, D. J. As, K. Lischka, T. Litz, A. Waag, T. Buhrow and F. Henneberger, *Phys. Rev. B* **54**, R8381 (1996).
14. P. Perlin, I. Gorczyca, N. E. Christensen, I. Grzegory, H. Teisseyre and T. Suski, *Phys. Rev. B* **54**, 13307 (1992).
15. M. A. Vidal, G. Ramirez-Flores, H. Navarro-Contreras, A. Lastras-Martinez, R. C. Powell and J. E. Greene, *Appl. Phys. Lett.* **68**, 441 (1996).
16. *Landolt Börnstein*, I. 4, II. 8, III. NS, Springer, Berlin.
17. S. Strite and H. Morkoç, *J. Vac. Sci. Technol. B* **10**, 1237 (1992).
18. M. H. Grimsditch and M. Cardona, *Phys. Status Solidi B* **102**, 155 (1980).